

KERNFORSCHUNGSZENTRUM

KARLSRUHE

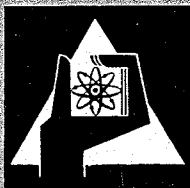
September 1967

KFK 678

Institut für Angewandte Kernphysik

Investigation of the Reaction $Dy^{164}(n, \gamma)Dy^{165}$

G. Markus, W. Michaelis, H. Schmidt, C. Weitkamp



GESELLSCHAFT FÜR KERNFORSCHUNG

KARLSRUHE

Investigation of the Reaction $\text{Dy}^{164}(n, \gamma)\text{Dy}^{165}$

G. MARKUS, W. MICHAELIS, H. SCHMIDT and C. WEITKAMP
Institut für Angewandte Kernphysik, Kernforschungszentrum Karlsruhe

Received June 19, 1967

The level structure of Dy¹⁶⁵ has been investigated at the Karlsruhe research reactor using thermal neutron capture in Dy¹⁶⁴. The target was Dy₂O₃ enriched to 92.71 % Dy¹⁶⁴. Neutrons were either monochromized by Bragg reflection from a lead crystal or transmitted through a bismuth single crystal filter. High-resolution measurements of the capture spectrum have been performed by means of a Ge(Li) 5-detector pair spectrometer and a Ge(Li) anti-Compton assembly. A large number of new lines has been observed. Cascade relationships were studied by using several techniques: a double coincidence apparatus with 4" \varnothing \times 5" NaI(Tl) detectors, a coincidence system containing a scintillation detector and a 34 cm³ Ge(Li)-diode as well as a two-parameter system involving the pair spectrometer (with NaI(Tl) as the primary detector) and a single 4" \varnothing \times 6" NaI(Tl) counter. In the framework of NILSSON's model and simple microscopic pictures of vibrational states the results are consistent with the following spectroscopic interpretation: 0 keV, 7/2⁺ [633]; 108.2 keV, 1/2⁻ [521]; 184.3 keV, 5/2⁻ [512]; 533.5 keV, 5/2⁻ [523]; 538.6 keV, 7/2⁺ [633] + Q₂₂; 570.3 keV, 5/2⁻ [512] + Q₂₂ + 1/2⁻ [510]; 573.6 keV, 3/2⁻ [521] + 1/2⁻ [521] + Q₂₂; 1103.3 keV, 1/2⁻ [521] + Q₂₂ + 3/2⁻ [521]. For comparison preliminary results are given for the isotonic nucleus Yb¹⁶⁹.

1. Introduction

Strongly deformed nuclei provide a good means to study both the effects of collective excitations and residual interactions of the nucleons¹⁻¹³ *. A typical odd-A deformed nucleus is Dy¹⁶⁵ which has an

* Bibliography, especially about theoretical approaches to the subject, is not exhaustive. Further references will be found in the literature cited.

¹ NILSSON, S.G.: Mat. Fys. Medd. **29**, 16 (1955).

² MOTTELSON, B.R., and S.G. NILSSON: Mat. Fys. Skr. **1**, 8 (1959).

³ NILSSON, S.G., and O. PRIOR: Mat. Fys. Medd. **32**, 16 (1961).

⁴ SOLOVIEV, V.G.: Mat. Fys. Skr. **1**, 11 (1961).

⁵ LIU YÜAN, N.I. PYATOV, V.G. SOLOVIEV, I. N. SILIN, and V.I. FURMAN: J. Exptl. Theoret. Phys. (U.S.S.R.) **40**, 1503 (1961).

⁶ BELYAEV, S.T.: Mat. Fys. Medd. **31**, 11 (1959).

⁷ MOTTELSON, B.R., and S.T. BELYAEV: The many body problem. New York: J. Wiley 1959.

⁸ MOSZKOWSKI, S.A.: Handbuch der Physik, Bd. XXXIX. Berlin-Göttingen-Heidelberg: Springer 1957.

⁹ SIEGBAHN, K. (Ed.): Alpha-, beta-, gamma-ray spectroscopy. Amsterdam: North Holland Publ. Co. 1965.

¹⁰ BROWN, G.E.: Unified theory of nuclear models. Amsterdam: North Holland Publ. Co. 1964.

¹¹ ALAGA, G., K. ALDER, A. BOHR, and B.R. MOTTELSON: Mat. Fys. Medd. **29**, 9 (1955).

¹² BOHR, A., and B.R. MOTTELSON: Phys. Rev. **90**, 717 (1953).

¹³ DIAMOND, R.M., B. ELBEK, and F.S. STEPHENS: Nuclear Phys. **43**, 560 (1963).

equilibrium deformation of $\delta \approx 0.32$. The investigation of the Dy^{165} level structure is essentially limited to the (n, γ) and (d, p) reactions on the target nucleus Dy^{164} . These reactions have been extensively studied with the Risø bent crystal spectrometer¹⁴ and magnetic spectrographs^{15,16}. As much as 220 neutron capture γ -rays were reported and 80 levels were obtained in (d, p) -measurements. From the high accuracy of the energy determination these authors were able to construct a level scheme for the excited states of Dy^{165} up to 650 keV applying RITZ' combination principle to the most prominent lines in the spectra.

In spite of these rather extensive studies the nature of the excited levels above 650 keV is still unknown. Thus it seems worthwhile to apply further techniques to this nucleus in order to refine and amplify the data on its level scheme. Preliminary results of this work were presented at the Antwerp Conference¹⁷ in 1965.

2. Experimental Procedure

2.1. Target

A sample of 100 mg Dy_2O_3 powder enriched to 92.71 % of Dy^{164} was pressed into a thin walled graphite cylinder of 6 mm internal diameter. The isotopic analysis of the target material is as follows:

Isotope	Atomic %	Isotope	Atomic %
Dy^{156}	< 0.02	Dy^{162}	1.34 ± 0.05
Dy^{158}	< 0.02	Dy^{163}	5.55 ± 0.05
Dy^{160}	< 0.02	Dy^{164}	92.71 ± 0.05
Dy^{161}	0.40 ± 0.05		

In the spectrographic analysis no lines were visible from other elements. Their admixture is definitely less than 0.1 %. Neutron capture in Dy^{164} thus accounts for about 98.7 % of the events observed, consistent with the above isotopic abundances and with the relative isotopic cross sections^{15,18}. Thus contributions of other isotopes in the Dy^{165} spectrum are negligible.

¹⁴ SCHULT, O. W. B., B. P. MAIER, and U. GRUBER: Z. Physik **182**, 182 (1964).

¹⁵ GROSHEV, L. V., A. M. DEMIDOV, V. N. LUTSENKO i V. I. PELEKHOV: Atomic Energy (U.S.S.R.) **4**, 5 (1958); Transl.: Atlas of gamma-ray spectra from radiative capture of thermal neutrons. London-New York: Pergamon Press 1959.

¹⁶ SHELIN, R. K., and W. N. SHELTON; MOTZ, H. T., and R. E. CARTER: Phys. Rev. **136**, 351 (1964).

¹⁷ MARKUS, G., W. MICHAELIS, H. SCHMIDT, and C. WEITKAMP: Proceedings of the Internat. Conference on the Study of Nuclear Structure with Neutrons. Amsterdam: North Holland Publ. Co. 1965.

¹⁸ Chart of the nuclides, 2nd edit. München: Gersbach & Sohn 1963.

Since the experiments described in this paper were performed with external target geometry the maximum fluxes are much lower than in previous (n, γ)-investigations which were carried out with the target near the core of the reactor. Neutron capture in Dy^{165} and built up of Ho^{165} can thus be neglected.

2.2. Thermal Neutron Beams

The experiments were performed at 2 horizontal channels of the Karlsruhe research reactor FR 2. In one case the beam from a core channel was monochromized by Bragg diffraction to a neutron wave length of approximately 1.2 Å (cf. ref. ^{19,20}). During these measurements the neutron flux at the target position was* $0.78 \times 10^6 \text{ cm}^{-2} \text{ sec}^{-1}$. The ratio of the thermal flux to the resonance flux per \log_e interval was found to be 26000. Most of the two-parameter experiments were performed at this channel.

For investigating the high-energy capture spectrum use was made of a 5-crystal pair spectrometer. This instrument was located at a tangential channel which passes through the heavy water of the reflector. Collimation of the neutron beam was done in such a way that the target was irradiated only by neutrons emerging from a 75 mm long 50 mm \varnothing graphite scatterer placed in the center of the channel. A bismuth single crystal filter of 20 cm length reduced the γ -radiation in the beam by a factor of 3×10^{-4} for the most penetrating radiation. The cadmium ratio behind the bismuth filter amounted to 7100. The thermal flux at the target position was $4.0 \times 10^6 \text{ cm}^{-2} \text{ sec}^{-1}$. After an increase of the reactor power the flux was found to be $3.3 \times 10^7 \text{ cm}^{-2} \text{ sec}^{-1}$. The flux was continuously monitored with a fission chamber. By means of a special control unit the measurements were stopped and restarted automatically when the flux dropped below or exceeded preset limits.

In section 3.2. preliminary results are given which were obtained by means of a Ge(Li) anti-Compton assembly. This spectrometer was one of 4 facilities placed at the same tangential through-hole, but at the opposite side of the reactor. The general arrangement was similar to that of the pair spectrometer. However, the bismuth filter was cooled to liquid nitrogen temperature and use was made of the total reflection of cold neutrons from a neutron guide tube. Thus the flux at the target position was somewhat higher than for the pair spectrometer in spite of a larger distance from the graphite scatterer.

* Due to an increase of the reactor power the flux is now about $3.5 \times 10^6 \text{ cm}^{-2} \text{ sec}^{-1}$.

¹⁹ WEITKAMP, C., W. MICHAELIS, H. SCHMIDT u. U. FANGER: Z. Physik **192**, 423 (1966).

²⁰ SCHMIDT, H., W. MICHAELIS, C. WEITKAMP u. G. MARKUS: Z. Physik **194**, 373 (1966).

2.3. Apparatus

The high-energy part of the γ -ray spectrum and coincidence relationships involving high-energy transitions have been investigated with a five-crystal pair spectrometer. The geometric arrangement of this instrument is shown in Fig. 1. γ -rays from the target were filtered through 4 mm of lead and collimated by a 45 mm long conical lead collimator onto the primary detector. The distance of the detector center from the target axis was 110 mm. The spectrometer can be operated both with a lithium-drifted germanium diode and a NaI(Tl) scintillator as the primary detector. In the measurements described in this paper the germanium counter had a sensitive volume of $2.7 \text{ cm}^2 \times 0.2 \text{ cm}$. Gamma rays were incident on the cylindrical surface of the detector. The scintillator was a $1'' \text{ } \varnothing \times 1.5''$ crystal connected via a cylindrical light pipe of polished plexi-glass to a RCA 6810 A photomultiplier. The secondary detectors consisted of 4 wedge shaped $3'' \text{ } \varnothing \times 3''$ NaI(Tl) crystals. They were mounted on RCA 6810 A type photomultipliers. Scattered neutrons from the target were kept off the detectors by a double walled polyethylene tube filled with 8 mm of packed Li^6H powder. Each of the secondary detectors was shielded by at least 3 cm of lead against direct radiation from the target. Typical resolution of the pair spectrometer when operated with a germanium counter was 10–15 keV FWHM* including long term instabilities.

Due to the external target geometry the pair spectrometer is capable of two-parameter coincidence measurements when the fore-mentioned scintillation counter is used as the primary detector. The coincident γ -rays were detected with a single $4'' \text{ } \varnothing \times 6''$ NaI(Tl) crystal mounted on a RCA 7046 photomultiplier. The distance of this detector from the target was continuously variable from 13 to 42 cm. In order to prevent counter-to-counter scattering the detector axis was placed at an angle of 120° to the axis of the pair spectrometer.

The gamma-ray spectrum in the energy range from 600 keV to 2300 keV was investigated using a Ge(Li) anti-Compton spectrometer. A detailed description of this apparatus is given in ref. ²¹ (see also ref. ^{22,23}). The energy resolution was 2.15 keV FWHM for the 662 keV Cs^{137} gamma ray.

* By using a charge sensitive preamplifier with paralleled field-effect transistors at 140°K the resolution is now considerably improved. In addition the efficiency will be increased by about one order of magnitude using a germanium diode with larger sensitive volume.

²¹ MICHAELIS, W., and H. KÜPPER: Nuclear Instr. and Meth. (to be published).

²² MICHAELIS, W., and H. SCHMIDT: KFK 429 (1966); Proc. of a IAEA Panel, Vienna, 6–10 June 1966.

²³ MICHAELIS, W., U. FANGER, D. LANGE, G. MARKUS, H. SCHMIDT, and C. WEITKAMP: KFK 562 (1967).

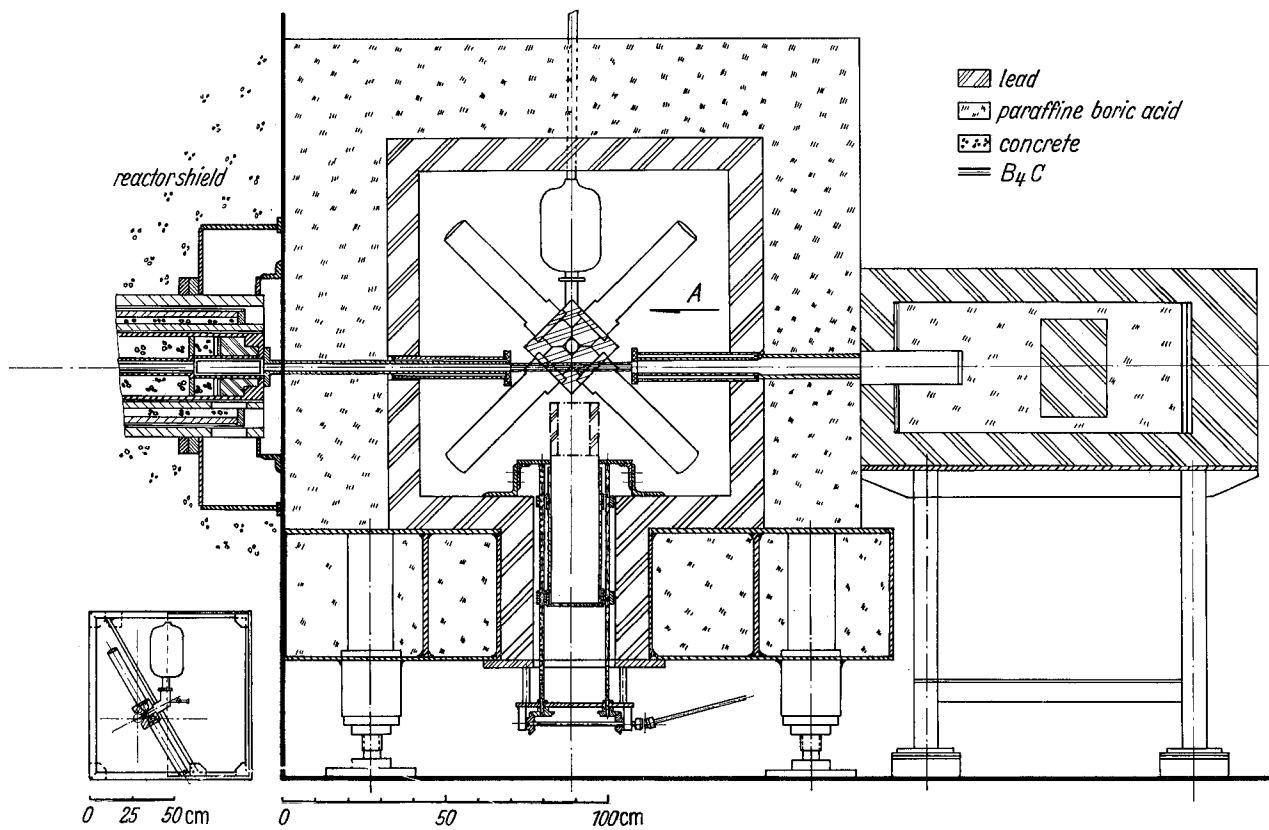


Fig. 1. Geometric arrangement of the pair spectrometer

Double coincidence measurements were performed using either two $4'' \text{ } \varnothing \times 5''$ NaI(Tl) crystals or one $3'' \text{ } \varnothing \times 3''$ scintillation detector in coincidence with a lithium-drifted germanium diode. The NaI(Tl) crystals were mounted on XP 1040 or RCA 8054 photomultipliers. The germanium diode was a coaxial detector with a sensitive volume of about 34 cm^3 . Using a preamplifier with paralleled field-effect transistors²⁴ at a temperature of $140 \text{ }^\circ\text{K}$ the energy resolution was 4.8 keV FWHM for the photopeak of the Cs^{137} $662 \text{ keV } \gamma$ -ray. The geometric arrangement and details of the apparatus for these measurements are described in ref.¹⁹. In several cases the double-window technique was applied in order to correct for the coincident background under the peak selected by the window in the gating branch of the coincidence system.

2.4. Electronics

The electronic systems used in the present experiments were of the conventional fast-slow coincidence type. Effective resolving times for

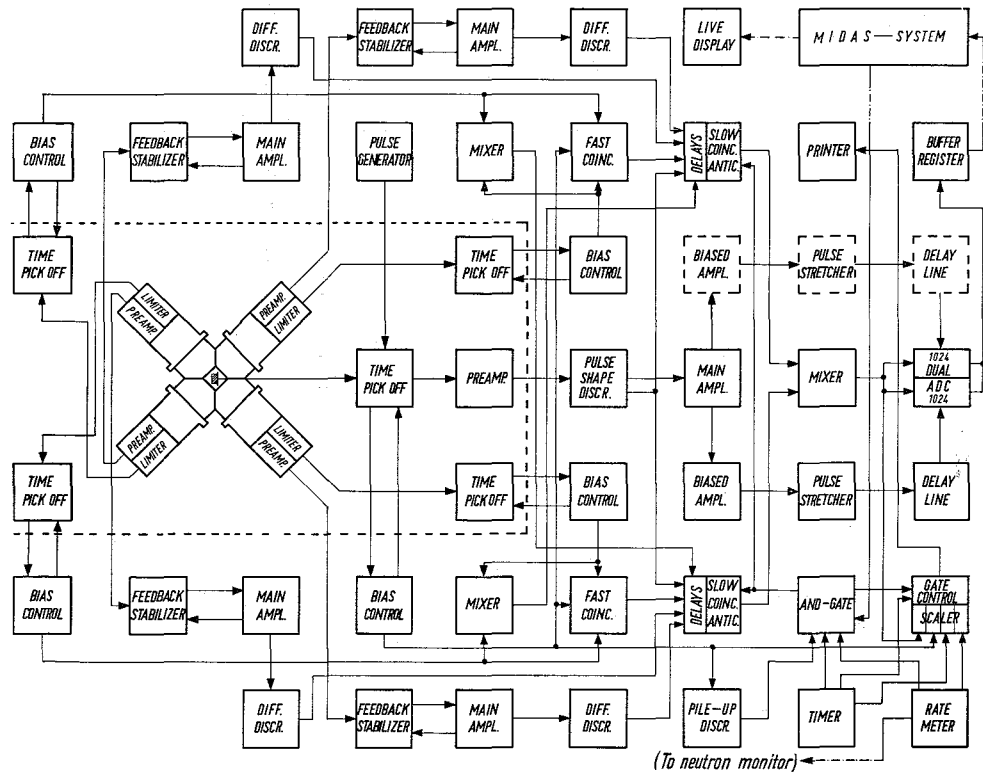


Fig. 2. Block diagram of the pair spectrometer

the fast coincidence circuits were between 20 and 100 nsec thus limiting the accidental coincidence rate to less than 1%. Slow coincidence resolving times were between 0.5 and 1 μ sec. Pulse pile-up was minimized to about 1% either by double delay-line clipping with clipping times of 0.7 μ sec or 1.2 μ sec for the scintillation detectors or by means of special time inspector anticoincidence units for the semiconductor detectors. More details about the electronic components may be found in refs. ^{19-21, 24, 25} and the literature cited there. Fig. 2 gives a block diagram of the pair spectrometer electronics.

2.5. Background and Energy Calibration

In the low-energy region background consisted mainly of 2223 keV capture γ -rays from neutron capture in polyethylene and the ever present 511 keV positron annihilation radiation. Above 2223 keV the background spectrum was essentially a continuum and decreased very rapidly with increasing energy. In the pair spectrometer measurements the contribution of the background to the counting rate was negligible.

Energy calibration was based on the annihilation peak and on the γ -line from the reaction $H(n, \gamma)D$. The linearity was carefully checked with a high precision mercury switch pulser. For calibrating the high-energy spectra obtained with the pair spectrometer the energy values for the most intense γ -rays were adopted from ref. ¹⁶.

2.6. Data Processing

Data accumulation was done either by means of conventional pulse height analyzers or by using the Karlsruhe on-line computer system (MIDAS)^{26, 27}. When long measuring periods were needed, the spectra were taken in short runs and made compatible afterwards by means of a special IBM 7074 program. Data handling in coincidence experiments with the on-line computer system is described in some detail in ref. ¹⁹.

3. Results

3.1. High-Energy Gamma-Ray Spectrum

The spectrum of high-energy gamma rays as obtained with the pair spectrometer is shown in Figs. 3 and 4. The results are summarized in Table 1. Due to the high capture cross section contribution of Dy¹⁶⁴ in the target material practically all clearly observed lines can be inter-

²⁴ TAMM, U.: KFK 509 (1967).

²⁵ TAMM, U., W. MICHAELIS, and P. COUSSIEU: Nuclear Instr. and Meth. **48**, 301 (1967).

²⁶ KRÜGER, G., and G. DIMMLER: KFK 242 (1964).

²⁷ KRÜGER, G.: Atomwirtschaft **10**, 118 (1965).

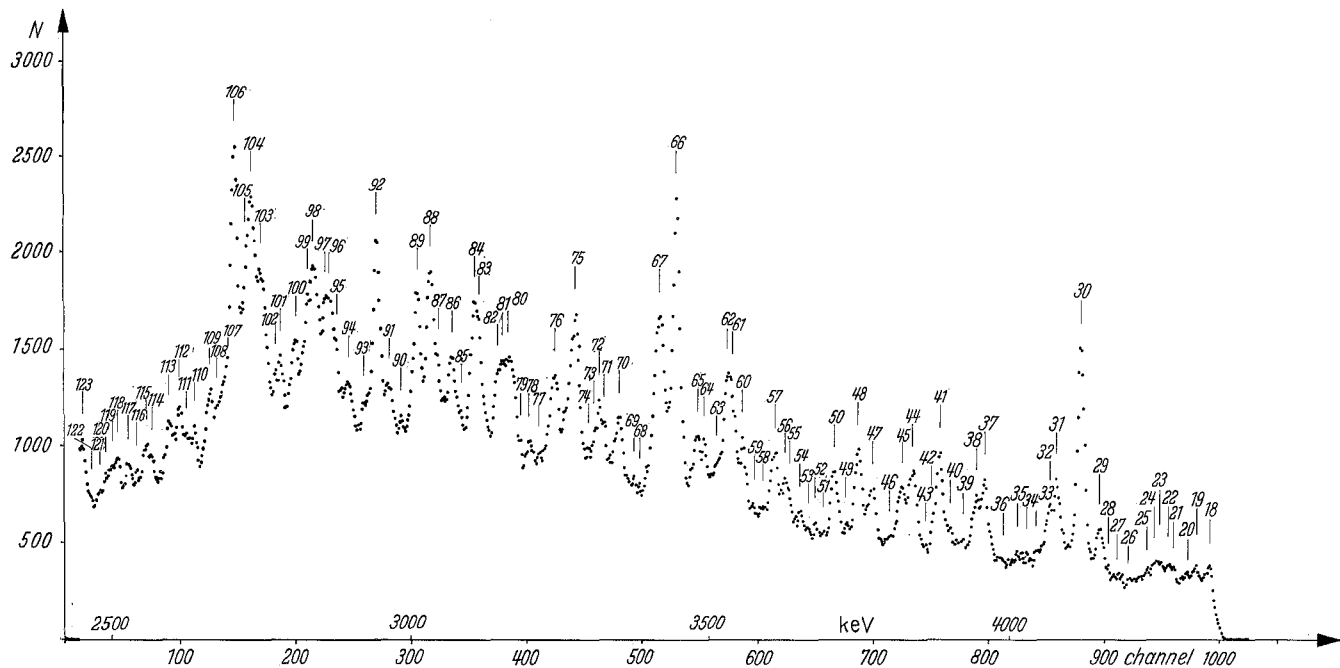


Fig. 3. High-energy gamma-ray spectrum from thermal neutron capture in 92.71% enriched Dy^{164} observed with the pair spectrometer. Energy range 2400 keV—4400 keV. The line numbers correspond to those given in Table 1

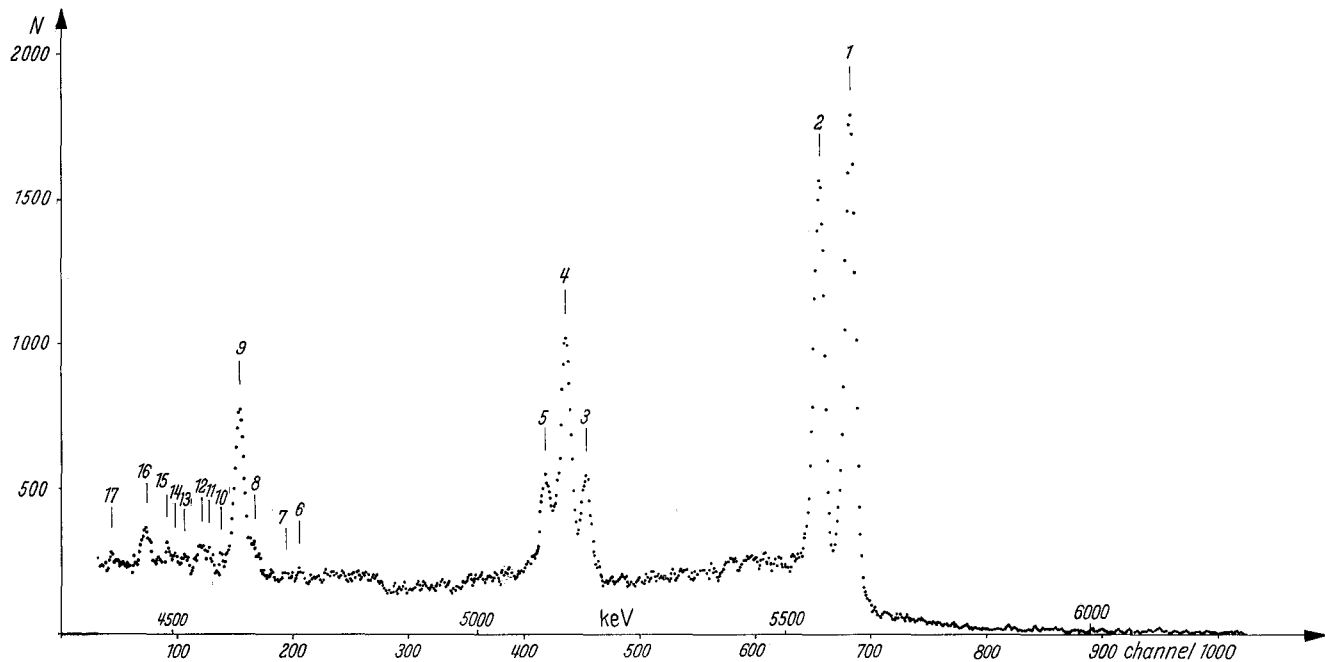


Fig. 4. High-energy gamma-ray spectrum from thermal neutron capture in 92.71% enriched Dy^{164} observed with the pair spectrometer. Energy range 4400 keV—6200 keV. The line numbers correspond to those given in Table 1

Table 1. Gamma rays from thermal neutron capture in 92.71% enriched Dy^{164} measured with a $Ge(Li)$ central detector in a five-crystal pair spectrometer. Energies are given in keV. Relative intensities are normalized to 100 for the most intense line in each of the 3 subgroups of this table

Line number	E [keV]	$\pm \Delta E$ [keV]	I	$\pm \Delta I$
1 c*	5606.7	0.2	100	—
2 c	5556.4	0.3	80	15
3	5175	2	13	3
4 c	5142.6	0.5	29	6
5	5109	2	10	2
6 u	4708	5	<1.5	
7 u	4684	5	<1.5	
8	4633	5	2.1	0.6
9	4612	2	12	2
10	4579	3	1.3	0.7
11	4559	4	1.6	0.8
12	4547	4	2.1	0.6
13	4522	5	1.3	0.7
14 u	4504	4	<1.5	
15	4491	4	1.9	1
16 d	4462	4	3	1
17 u	4420	4	<1.5	
18	4335	10	9.2	5
19	4314	4	9.2	5
20 u	4297	4	<7	
21	4278	4	<9	
22	4266	4	9.2	5
23	4256	4	<9	
24	4246	4	<9	
25	4231	4	<7.5	
26 u	4202	4	<4	
27 pd	4183	5	<5	
28 u	4167	5	<9	
29	4152	3	20	7
30 c	4123.2	0.4	83	17
31	4081	2	21	7
32	4069	3	16	8
33 u	4046	4	<8	
34	4031	5	8	4
35	4018	5	8	4
36	3987	5	<8	
37	3960	2	25	8
38	3947	3	19	7
39	3923	4	7.5	4
40	3902	4	7.5	4
41 c	3885.2	1	35	11
42 u	3873	5	<7.5	

* Legend: c=calibration line, u=uncertain line, d=doublet, pd=possible doublet.

Table 1 (Continued)

Line number	E [keV]	$\pm \Delta E$ [keV]	I	$\pm \Delta I$
43 u	3858	5	<7.5	
44 d	3841	3	27	9
45 $\frac{1}{2}$	3821	3	20	7
46 $\frac{1}{2}$ pd	3800	5	6.4	4
47 $\frac{1}{2}$ d	3772	4	20	7
48 $\frac{1}{2}$	3749	2	32	10
49 $\frac{1}{2}$	3727	4	7	4
50	3708	3	26	8
51 u	3689	5	<6	
52 $\frac{1}{2}$	3677	4	6	3
53	3664	4	6	3
54	3651	4	10	5
55 u	3633	5	<11	
56	3626	3	13	7
57 pd	3610	4	27	9
58 $\frac{1}{2}$ pd	3588	5	7	4
59	3672	4	7	4
60	3555	3	29	9
61	3534	3	} 50	} 16
62	3528	3		
63	3511	4	<15	
64	3490	3	21	10
65	3478	3	21	10
66	3445	2	100	—
67 pd	3417	3	56	18
68 u	3383	5	<7	
69	3374	4	<7	
70	3349	3	25	8
71	3323	4	15	6
72	3315	3	20	8
73 u	3309	5	<7	
74 u	3297	5	<7	
75 pd	3276	2	53	11
76 pd	3242	4	27	9
77	3216	4	<5	
78 pd	3199	4	9.7	5
79 u	3182	5	<8.5	
80 $\frac{1}{2}$ pd	3165	4	34	17
81	3153	4	26	13
82	3146	4	25	12
83	3114	3	39	16
84	3107	3	47	19
85	3084	4	11	5
86	3068	3	36	11
87	3047	5	21	10
88	3034	2	60	12
89	3012	2	44	9

Table 1 (Continued)

Line number	$E[\text{keV}]$	$\pm \Delta E[\text{keV}]$	I	$\pm \Delta I$
90	2983	3	6.8	3
91 d	2963	4	17	8
92 c	2948	1	71	14
93	2922	5	6	3
94 pd	2894	4	17	5
95	2874	4	24	12
96	2866	3	38	15
97	2859	3	37	15
98	2838	2	50	20
99	2828	3	24	12
100	2807	3	24	12
101	2782	4	20	10
102 u	2773	5	< 14	
103 pd	2751	4	44	22
104	2734	2	73	22
105 u	2723	5	40	20
106 c	2705	1	100	—
107	2690	5		
108	2675	5		
109	2665	4		
110	2638	4		
111	2626	5		
112	2613	3		
113	2596	4		
114	2567	4		
115	2557	4		
116 u	2542	5		
117	2529	4		
118	2510	4		
119	2502	4		
120 u	2491	5		
121	2480	5		
122 u	2466	5		
123	2452	4		

puted as originating from Dy^{165} . A large number of new lines has been observed. The uncertainties given for the gamma-ray energies do not include systematic errors involving calibration and nonlinearity. These errors are expected to amount to less than 2 keV. For determining the gamma-ray intensities the double escape peak efficiencies as calculated by DE CASTRO FARIA and LÉVESQUE²⁸ were used. The results of these authors had to be corrected for tangential irradiation of the detector.

²⁸ DE CASTRO FARIA, N. V., and R. J. A. LÉVESQUE: Nuclear Instr. and Meth. **46**, 325 (1967).

background under the peak in the gating branch. Underlined gamma rays are interpreted as being in coincidence with the 184 keV transition.

In Figs. 6 and 7 the original data with an energy scale of about 665 eV per channel are shown. For disclosing weak lines in regions where statistics remained poor the measured spectra were reduced by adding the contents of two or three adjacent channels and/or a smoothing procedure implying two or three channels was applied to the original spectra. This method can yield clearer results in many cases provided a careful handling and thorough comparison with the original data is done.

3.4. Coincidence Measurements with NaI(Tl)-Detectors

In a previous paper¹⁶ the binding energy of the last neutron was determined to be 5715 ± 4 keV under the assumption that the highest strong gamma ray feeds the well known 1.26 min isomeric state at 108 keV. This result was verified by a coincidence measurement with a window at 5600 keV. No prompt coincidences were observed.

Fig. 8 gives the coincidence spectra with electronic window settings on the photopeaks at 4120 keV and 4610 keV. In these measurements the coincident background under the peaks in the gating detector consisted

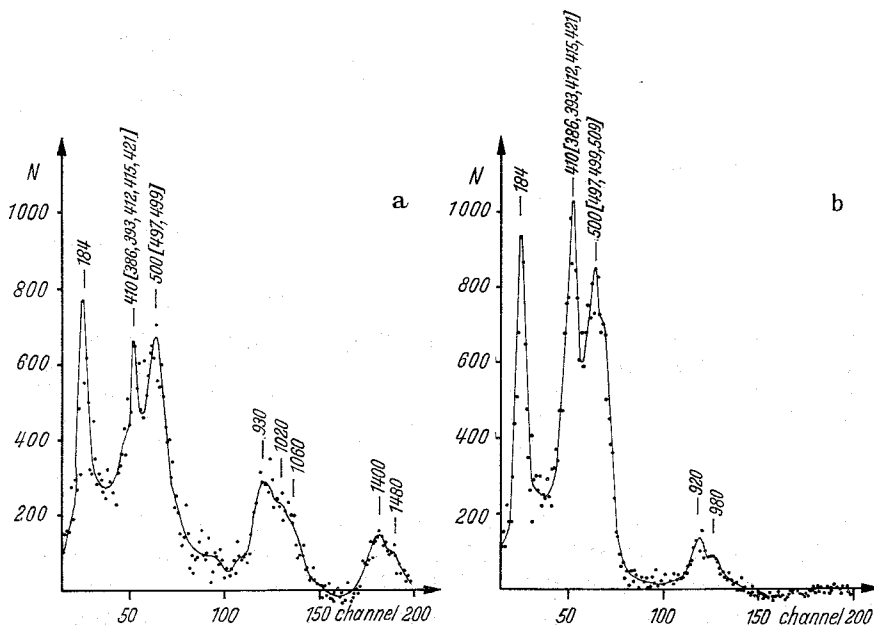


Fig. 8. Coincidence spectra taken with two $4'' \text{O} \times 5''$ NaI(Tl) detectors. The window settings in the gating branch were at a) 4120 keV and b) 4610 keV. Coincident background was subtracted by means of the double-window technique

mainly of single and double escape peaks from higher-energy gamma rays. Most of this background was subtracted by application of the double-window technique.

Gamma-gamma coincidence measurements in the low-energy region were performed with a major number of digital windows¹⁹ using the on-line computer system. All spectra were corrected for coincident background. A typical example is given in Fig. 9 which shows the pulse-

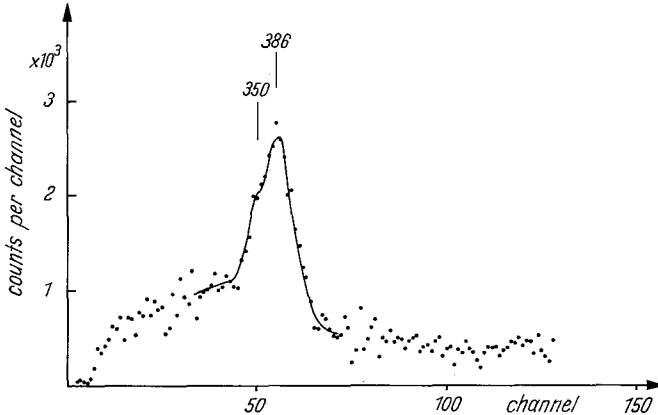


Fig. 9. Coincidence spectrum from neutron capture in Dy^{164} taken with two $4'' \text{ } \varnothing \times 5''$ NaI(Tl) detectors. MIDAS window at 184 keV

height distribution coincident to the 184 keV photopeak (cf. Fig. 7). Interference from other lines was clearly eliminated.

In many cases the interpretation of the NaI(Tl) coincidence spectra was made difficult by the poor resolution of these detectors. The precise knowledge of the singles spectra was of considerable aid in interpreting the results. When the assignment of the gamma-ray peaks found in the coincidence spectra or of the gamma rays within the window setting was not obvious, then the following criteria were used for deciding which gamma rays are responsible for the coincidence relationship: 1. the intensity of the lines in the relevant energy interval, 2. the energy difference between the NaI "group" and the nearest gamma lines observed with high-resolution instruments and 3. the "energy coincidence" of the resulting cascade.

3.5. Coincidence Measurements with the Pair Spectrometer

Coincidence studies were carried out with several digital windows¹⁹ in the high-energy spectrum using the on-line computer system. Though both resolution and statistics remain poor, such measurements have one feature that compensates in part for these disadvantages. There is no

contribution of secondary peaks of higher-energy transitions to the pulse height selected in the gating window. The method revealed no additional information, the results, however, supported various relationships obtained by means of other techniques.

4. Discussion

4.1. Level Scheme

The level diagram for Dy^{165} based on the results of the present investigation is shown in Fig. 10. Apart from the high-energy transitions proceeding from the capturing state only those gamma rays have been included which were observed in coincidence measurements. It is important to realize that coincidence studies provide the only means to construct a reliable decay scheme at higher excitation energies. A large number of additional gamma rays from Table 2 or from previous work can be fitted into the diagram using RITZ' combination principle. However, in most cases several level spacings are within present experimental errors in the gamma-ray energies. Thus when applying this procedure the position remains uncertain. Large dots in Fig. 10 indicate experimentally established coincidence relationships. Gamma rays entering a level and dotted at their arrowheads have been shown to be in coincidence with at least one gamma ray leaving the same level and dotted at its origin. The position of gamma rays not distinguished by dots is probable, but could not be definitely established. Dashed lines indicate transitions which remain uncertain for one of the following reasons: 1. The gamma-ray peak was not clearly resolved from neighbouring lines or 2. the coincidence spectra are consistent with fitting the relevant transition into the diagram at two different positions.

The interpretation of the high-energy gamma rays in Fig. 10 as primary transitions leaving the capture state is based mainly on energy and intensity considerations. Of course, the existence of the resulting levels has still to be confirmed by coincidence measurements. This is true, in particular, for the excited states at 2473, 2516, 2562, 2647, 2752 and 2841 keV. The occurrence of these levels is probable, but the evidence is not complete. A comparison of the level energies suggested by the present investigation with (d, p)-results is given in subsection 4.3. The error for the binding energy is assumed to be less than ± 3 keV.

The measurements described in this paper confirm the level scheme which was constructed previously¹⁴ for the energy range up to 650 keV by using the combination principle. This is, in particular, of importance for the bandheads at 534 and 570 keV since the evidence for the existence of these levels was not complete till now^{14, 16}. A level at 658 keV has already been observed in (d, p)-measurements¹⁶. Since the 570 keV state

was not detected in these studies, the 658 keV level was tentatively assigned in ref. ¹⁶ to a rotational band based on the Nilsson state $3/2^- [521]$ which was assumed to occur at 605 keV. The deexcitation of the 658 keV level is consistent with the spin value $5/2$, however, the (n, γ) data suggest that the levels at 605 keV and 658 keV are the second and third members of a rotational band with a $1/2^-$ bandhead at 570 keV. Using the bent crystal results from ref. ¹⁴ the exact energy value for the 658 keV state is calculated to be 657.98 ± 0.04 keV.

The level at 1103 keV most probably has spin and parity $3/2^-$. It is populated by a strong transition from the capturing state and deexcited to levels with spins $1/2$, $3/2$ and $5/2$. The reduced transition probabilities (cf. subsection 4.2) are consistent with this assignment. The new gamma rays postulated in our preliminary report¹⁷ have been established. From the low-energy transitions involved the exact level energy is calculated to 1103.31 ± 0.06 keV.

The existence of a level at 1167 keV has still to be confirmed by coincidence relationships which comprise gamma-ray transitions feeding this state. If the interpretation given in Fig. 10 is correct then the level should have positive parity and a spin value of $3/2$. This follows from internal conversion measurements which suggest the 509 keV gamma ray to be $E1$ radiation³⁰.

A level at 1590.9 ± 0.6 keV is well established by the coincidence results. Most probably, spin and parity are $3/2^-$. Odd parity states with spin values $1/2$ or $3/2$ occur at 1563 keV and 1646 keV, respectively.

Besides the energy levels shown in Fig. 10 some evidence was found for the existence of several levels with excitation energies between 650 keV and 1103 keV. However, the data are not yet conclusive and further coincidence measurements are required.

4.2. Reduced Transition Probabilities

In Table 3 the experimental ratios of reduced transition probabilities are compared with the theoretical predictions for several levels in Dy¹⁶⁵. According to ALAGA¹¹ these ratios depend only on geometrical factors when the emission of radiation from a state i to different members f, f' of a rotational family is considered. The general rule can be written in the form

$$\frac{B(L, J_i \rightarrow J_f)}{B(L, J_i \rightarrow J_{f'})} = \left[\frac{\langle J_i L K_i K_f - K_i | J_i L J_f K_f \rangle}{\langle J_i L K_i K_f - K_i | J_i L J_{f'} K_{f'} \rangle} + \frac{b(-1)^{J_f + K_f} \langle J_i L K_i, -K_f - K_i | J_i L J_f - K_f \rangle}{+ b(-1)^{J_{f'} + K_{f'}} \langle J_i L K_i, -K_{f'} - K_i | J_i L J_{f'} - K_{f'} \rangle} \right]^2,$$

³⁰ BONDARENKO, V. A., P. T. PROKOFIEV i L. I. SIMONOVA: Izv. Akad. Nauk S.S.S.R., Ser. Fiz. **29**, 12, 2168 (1965); — Bull. Acad. Sci. U.S.S.R., Phys. Ser. **29**, 12, 2004 (1965).

where b is a parameter depending on the intrinsic wave functions. When either K_i or K_f is zero or when $L < K_i + K_f$, the second terms both in the numerator and the denominator of this expression vanish.

Of particular interest is the deexcitation of the $1/2^-$ $K=2$ gamma vibrational band to the levels of the $1/2^-$ [521] rotational family. In Table 3 the theoretical branching ratios are given for $M1$ radiation assuming different values of b and for $E2$ radiation with $b=0$. A value $b=0.91$ was proposed in ref. ¹⁴ for fitting the observed intensities of transitions leaving the levels at 570 and 605 keV. Unfortunately only one strong gamma ray has been detected till now from each of these states. For the intensities of other possible transitions only upper limits can be given. Thus the parameter b deduced from these levels remains somewhat arbitrary and the data are not very conclusive. If the two transitions, now identified as deexciting the third rotational member at 658 keV (cf. Fig. 10), are assumed to be pure $M1$ radiation, from the branching ratio a value of 0.785 can be calculated for b . However, none of the values $b=0$, 0.785 and 0.91 gives a satisfactory fit to the experimental data. Even the assumption of $E2$ admixtures in the relevant radiations cannot improve the agreement. The above formula for the reduced transition probabilities was derived for transitions between states which can be represented by pure wave functions of the simple product type. The results in Table 3 suggest that this assumption is not valid in the case considered here.

Along with the 519 keV transition from the 1103 keV level to the $5/2^+$ member of the $3/2^+$ rotational band, a transition with comparable intensity is expected reaching the $3/2^+$ bandhead. This is consistent with the probable existence of a 538 keV – 565 keV coincidence relationship. Thus we can conclude that the gamma ray at 565.16 keV is a closely spaced doublet, one component leaving the level at 649 keV, in agreement with ref. ¹⁴, the other one proceeding from the 1103 keV state. It is worth-while to note that this conclusion may eliminate to some extent the discrepancy which arises when calculating the exact energy of the 649 keV level from the transitions within the rotational sequence and from the transitions going to the ground-state rotational band (cf. ref. ¹⁴). The expected energies for the two components are 564.69 keV and 565.56 keV, respectively, and may well give a centroid at 565.16 keV. The energy difference is less than the minimum spacing which is required for clearly resolving in 5th reflexion order two lines of equal intensity.

4.3. Comparison with (d, p) Results

Table 4 gives a comparison of the level energies obtained in the present investigation with (d, p) measurements from ref. ¹⁶. For the levels up to

Table 3. *Reduced transition probabilities*

Level E_i [keV]; $J_i \pi_i K_i$	$K_f \pi_f$	$J_f J_{f'}$	$\frac{B(L; E_\gamma)}{B(L; E_{\gamma'})}$	Theory	Experiment
570; $1/2^- 1/2$	$1/2^-$	$3/2 1/2$	$\frac{B(M1; 412)}{B(M1; 462)}$	2.0 ($b=0$) 400 ($b=0.785$) 65 ^a ($b=0.91$)	> 22
			$\frac{B(M1; 446)}{B(M1; 497)}$	0.20 ($b=0$) 0.86 ($b=0.785$) 0.95 ^a ($b=0.91$)	< 0.2
605; $3/2^- 1/2$	$1/2^-$	$3/2 1/2$	$\frac{B(E2; 446)}{B(E2; 497)}$	1.0 ($b=0$)	< 0.091
			$\frac{B(M1; 424)}{B(M1; 497)}$	1.8 ($b=0$) 0.15 ($b=0.785$) 0.085 ^a ($b=0.91$)	
			$\frac{B(E2; 424)}{B(E2; 497)}$	0.43 ($b=0$)	
	$5/2^-$	$7/2 5/2$	$\frac{B(E2; 343)}{B(E2; 421)}$	0.75	1.1
658; $5/2^- 1/2$	$1/2^-$	$5/2 3/2$	$\frac{B(M1; 477)}{B(M1; 499)}$	0.071 ($b=0$) 2.0 ($b=0.785$) 4.6 ($b=0.91$)	2.0 ^b
			$\frac{B(E2; 477)}{B(E2; 499)}$	4.0 ($b=0$)	
			$\frac{B(M1; 360)}{B(M1; 499)}$	1.4 ($b=0$) 17 ($b=0.785$) 30 ($b=0.91$)	< 0.3
	$7/2 3/2$	$\frac{B(E2; 360)}{B(E2; 499)}$	0.67		
		$\frac{B(E2; 396)}{B(E2; 474)}$	2.4	> 2.5	
1103; $3/2^- 3/2$	$1/2^-$	$3/2 1/2$	$\frac{B(M1; 945)}{B(M1; 995)}$	0.80	0.54
			$\frac{B(M1; 921)}{B(M1; 995)}$	0.20	0.63 ^c
	$3/2^-$	$5/2 3/2$	$\frac{B(M1; 475)}{B(M1; 530)}$	0.67	> 1.5 ^d
			$\frac{B(E2; 475)}{B(E2; 530)}$	2.6	
	$3/2^+$	$5/2 3/2$	$\frac{B(E1; 519)}{B(E1; 565)}$	0.67	> 0.5 ^e
1591; $3/2^- 3/2$	$3/2^-$	$5/2 3/2$	$\frac{B(M1; 962)}{B(M1; 1017)}$	0.67	< 0.3

Table 4. Dy^{165} levels. Comparison with (d, p) results

$(n, \gamma)^a$ [keV]	$(d, p)^b$ [keV]	$(n, \gamma)^a$ [keV]	$(d, p)^b$ [keV]	$(n, \gamma)^a$ [keV]	$(d, p)^b$ [keV]
83.4	84.5		1506		2373
108.2	108.2	1563	1563		2432
158.6	158.4	1591		2439	
180.9	180.7		1598		2445
184.3		1634			2459
186.1		1646	1652	2473	
261.8	261.5	1697	1700	2499	2495
297.7 ^c	296.3	1728	1725	2516	
337.2 ^c	336.9	1755	1753		2524?
360.6 ^c	360.5	1768		2550	
480.1 ^c	480	1830	1835	2562	
520.5 ^c	519		1863	2569	
533.5	537 ^d	1874			2576
538.6		1894	1893	2601	2596
570.3	574 ^d		1920	2608	
573.6		1942			2620
584.0			1949	2647	
605.1	605	1966	1971		2657
628.8	629	2007	2006	2681	
649.0 ^c			2029	2703	2704
658.0	658	2064	2069		2741
	707		2076	2752	
	773		2098	2767	
	884	2105		2793	2792
	919	2127	2124		2815
	1054		2152	2821	
1103.3	1106	2160			2834
	1145	2181	2179	2841	
1167.0	1166	2187		2856	2859
1253		2204	2209	2877	
	1262	2225	2230		2899
	1316	2237			2920
	1343		2247		2948
	1389	2270	2268	2964	
1401	1407		2288	2981	
1449	1452	2298		3010	3006
1469			2323		3016
		2366		3025	

^a This work. ^b From ref.¹⁶. ^c Taken from ref.¹⁴. ^d Possible doublet.

^a These values differ from the theoretical branching ratios calculated in ref.¹⁴ for $b=0.91$.

^b The value $b=0.785$ was fitted to this branching ratio.

^c The line observed at 921 keV is possibly a doublet.

^d Possibly perturbed by complex structures of the gamma-ray spectrum.

^e The 565.16 keV gamma line (cf. ref.¹⁴) most probably consists of two closely spaced components (see text).

649 keV more precise energy values may be taken from the bent crystal results¹⁴.

4.4. Spectroscopic Interpretation

It is well known from a large number of studies that the level density predicted by the pure Nilsson model is lower than that observed experimentally. Much better agreement is achieved when the effects of residual interaction are taken into account. Calculation for Dy¹⁶⁵ including pairing correlations have been reported in ref. ⁴. A further complication is introduced by the coupling of the single-particle motion to collective modes of excitation. The spacings of single-particle states are such that levels connected by large $E2$ matrix elements occur separated by approximately the quadrupole phonon energy. Strong coupling of these motions therefore is very probable. A break-down of the pure single-particle description and a considerable mixing are expected. Some of the phenomena are best understood in a simple microscopic picture of the vibrational states. In this picture the vibrational excitations are described as superpositions of one-quasiparticle and three-quasiparticle states. The three-quasiparticle states consist of the unpaired particle of the odd nucleus, characterized by the spin component K_0 , and of the various two-quasiparticles with K and $K \pm 2$ which make up the quadrupole vibration of the even nucleus. A special case is the strong connection of the state K_0 with states $K_0 \pm 2$ by large $E2$ matrix elements. The configurations of the even nucleus gamma vibrations will involve a quasiparticle with $-K_0$ and in the odd nucleus single-particle states $K_0 \pm 2$ will be admixed into the vibrational wave function. Noticeable admixtures of such states require that the selection rules in the asymptotic quantum numbers $[Nn_z A]$ are fulfilled: $\Delta N = 0$ (or ± 2), $\Delta n_z = 0$ and $\Delta A = 2$. Otherwise the $E2$ matrix element vanishes. Similar arguments may be applied to the octupole vibrations, though the effects are expected to be much smaller than in the quadrupole case.

From these considerations one can conclude that the $K-2$ gamma vibrational band based on the $1/2^-$ [521] state contains the component $3/2^-$ [521] and vice versa. Similarly, the $1/2^-$ [510] state should be admixed to the $K-2$ vibration on the $5/2^-$ [512] state. For the low-energy levels the admixtures are expected to be small and these states should be nearly pure quasiparticle configurations. The first $3/2^+$ state is essentially collective in nature since the levels which give reasonable $E2$ matrix element strengths occur at relatively high excitation energies.

tonic species Dy¹⁶⁵, Er¹⁶⁷ and Yb¹⁶⁹. Only the dominant admixture is given for each level. The data concerning Er¹⁶⁷ and Yb¹⁶⁹ have also been obtained by radiative neutron capture at the Karlsruhe research reactor and will be published in the near future. In general, the agreement between theory and experiment is surprisingly good. A striking feature of the quasiparticle-phonon interaction is the appearance of large components of high-lying Nilsson states in the low-energy region. A typical example is the admixture of the $1/2^-$ [510] state into the $K=2$ vibration on the $5/2^-$ [512] state. Theoretically an amplitude of about 30% is predicted. The occurrence of a non-vanishing decoupling parameter for the corresponding rotational band may be ascribed to such an admixture. The experimental value $a=0.048$ for Dy¹⁶⁵ coincides very well with the theoretical prediction $a=0.05$. The results obtained for Er¹⁶⁷ and Yb¹⁶⁹ are in favour of this spectroscopic interpretation. Obviously, the contribution of the $1/2^-$ [510] state seems to increase from Dy¹⁶⁵ to Yb¹⁶⁹. For comparison in Fig. 12 a preliminary transition diagram for Yb¹⁶⁹ is shown which was deduced from a coarse analysis of the low-energy spectrum measured with the anti-Compton spectrometer. The rotational band in question occurs at 806.9, 851.2 and 912.0 keV. From these energies the decoupling parameter and the rotational factor are calculated to $a=0.097$ and $\hbar^2/2\theta=13.5$ keV, whereas the rotational factor for the $5/2^-$ [512] band is 12.4 keV. Thus we are forced to conclude that the $1/2^-$ state cannot be characterized by a pure vibrational wave function. A further indication of the above mixed configuration is provided by the intensities observed in (d, p) reactions (cf. subsection 4.1). In the picture sketched above the experimental population can be well understood.

In the light of these theoretical aspects the hitherto accepted interpretation of the $3/2^-$ bandhead at 574 keV as the $K=2$ vibrational state based on the $1/2^-$ [521] Nilsson orbital must be revised. Most probably, the 574 keV level is predominantly the quasiparticle state $3/2^-$ [521]. The theoretical calculations³⁰ revealed a contribution of 68%. The $3/2^-$ state with a prevailing vibrational character (89%) occurs at 1103 keV. The energies of both states are in satisfactory agreement with the theoretical prediction. Unfortunately the inertial parameters for the orbitals $3/2^-$ [521] and $1/2^-$ [521] are very similar. Thus a comparison of these parameters for the rotational bands in question is irrelevant.

While the first $3/2^+$ state in Dy¹⁶⁵ is mainly collective, the corresponding state in Yb¹⁶⁹ is predominantly the quasiparticle state $3/2^+$ [651]. This is predicted theoretically^{30, 31} due to an energy increase of the gamma vibrational excitations in Yb¹⁶⁸ as compared to Dy¹⁶⁴ and Er¹⁶⁶. Experimentally this change in structure can be deduced from the probably pronounced change of the inertial parameter (the rotational levels are not shown in Fig. 12).

If the existence of a $3/2^+$ level at 1167 keV can be confirmed, this state may have the structure³¹ $3/2^+$ [651]; $3/2^-$ [521] + Q_{30} . Some of the weak high-energy transitions observed between 4500 keV and 4800 keV possibly correspond to dipole transitions from the capturing state to excited levels with the following dominant components: $5/2^+$ [642] + Q_{22} and $5/2^-$ [523] + Q_{22} . These configurations are expected between 900 keV and 1100 keV. From energy considerations alone the 1253 keV state may belong to the rotational band characterized by the structure $5/2^-$ [523] + Q_{32} . For obtaining reliable information on the nature of these states further coincidence studies are required. Experiments applying improved techniques are in progress.

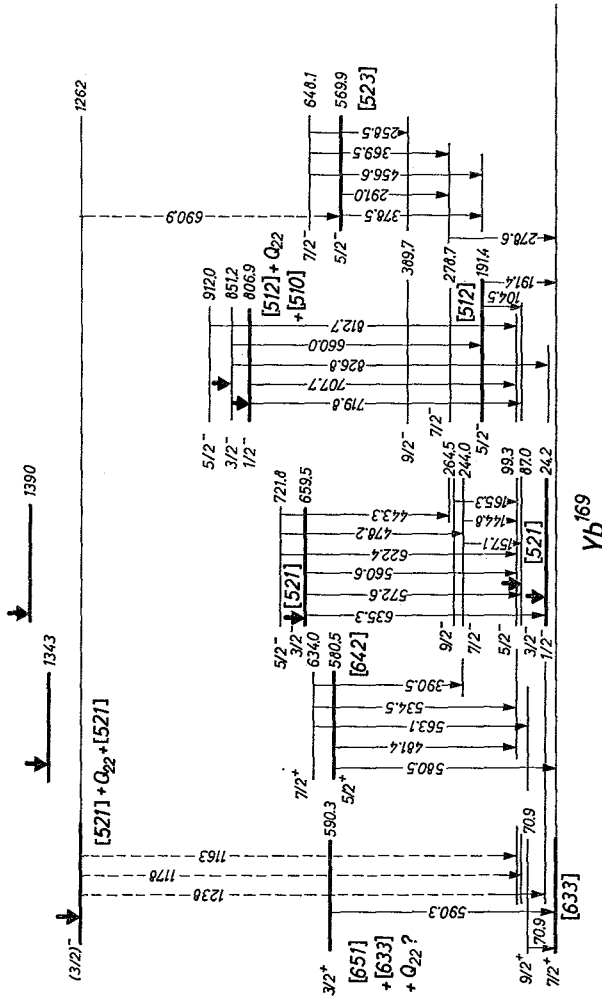


Fig. 12. Transition diagram for Yb^{169} (preliminary data). Large arrows indicate primary transitions from the capturing state

Note added in proof: Following the completion of the manuscript we got knowledge of a conversion electron investigation^{33,34} of neutron capture in Dy^{164} . Using the observed multipolarities and previously known transition energies the authors have constructed a transition diagram for the product nucleus. In the low-energy region this diagram is in full agreement with that given in the present paper. At higher excitation energies some discrepancies exist which clearly demonstrate the need for more precise energy values and further coincidence studies.

³³ V. EGIDY, T., H.F. MAHLEIN, W. KAISER, B.C. DUTTA, A. JONES, and A.A. SUAREZ: Diskussionstagung über Neutronenphysik an Reaktoren, Jülich, 25. April 1967.

³⁴ DUTTA, B.C., T. V. EGIDY, TH. W. ELZE, and W. KAISER: Z. Physik (to be published).